Broadband THz detection and homodyne mixing using GaAs high-electron-mobility transistor rectifiers

S. Preu[a,1], S. Regensburger[a], S. Kim[b], M. Mittendorff[c], S. Winnerl[c], S. Malzer[a], H. Lu[d], P. G. Burke[d], A.C. Gossard[d], H.B. Weber[a], and M.S. Sherwin[d]

[a]Chair for Applied Physics, University of Erlangen-Nuremberg, Erlangen, Germany
[b]Tanner Research, Monrovia, CA 91016 USA.
[c]Helmholtz-Zentrum Dresden-Rossendorf, Dresden, Germany
[d]Univ. of California, Santa Barbara, 93106 Santa Barbara, CA, USA

ABSTRACT

We report on Terahertz (THz) detectors based on III-V high-electron-mobility field-effect transistors (FET). The detection results from a rectification process that is still highly efficient far above frequencies where the transistor provides gain. Several detector layouts have been optimized for specific applications at room temperature: we show a broadband detector layout, where the rectifying FET is coupled to a broadband logarithmic-periodic antenna. Another layout is optimized for mixing of two orthogonal THz beams at 370 GHz or, alternatively, 570 GHz. A third version uses a large array of FETs with very low access resistance allowing for detection of very short high-power THz pulses. We reached a time resolution of 20 ps.

Keywords: THz detection, field effect transistor, ultrafast detector, mixing

1. INTRODUCTION

Within the last decade, Terahertz (100 GHz-10 THz) radiation became a very attractive tool for many applications due to its unique properties: it is non-ionizing, i.e. not harmful at typical power levels and it penetrates through many common materials such as paper envelopes or clothing. Applications include spectroscopy [1] with capabilities to analyze the isotopic composition [2], imaging and security. Particularly for the detection of harmful chemicals such as drugs or

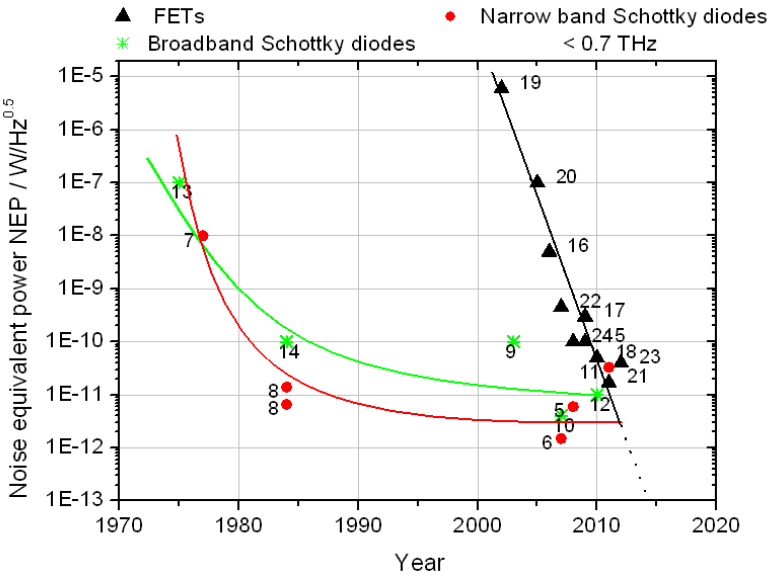

Fig. 1: Comparison of the NEP for direct detection of room-temperature operating Schottky diodes[2]below 0.7 THz [5-14] and field effect transistor rectifiers [15-24]. The solid lines are guides for the eye.

[1] sascha.preu@fau.de; phone: +49/9131/85-28696; fax: +49/9131/85-28423

Millimetre Wave and Terahertz Sensors and Technology VI, edited by Neil Anthony Salmon, Eddie L. Jacobs,
Proc. of SPIE Vol. 8900, 89000R · © 2013 SPIE · CCC code: 0277-786X/13/$18 · doi: 10.1117/12.2029478

explosives [3] THz radiation has proven to be very useful. Besides a tunable source, such as photomixers [4], low noise detectors with fast data acquisition rates are required. For most applications, both detectors and sources must work at room temperature in order to reduce system cost and complexity. Fast, room temperature operating detectors include Schottky diodes [5-14] and field-effect transistor rectifiers (FETs) [15-34]. Schottky diodes have been developed over decades and reached a very sophisticated technological level. Noise equivalent powers are in the range of few pW/√Hz [6]. Rectifying FETs currently reach noise floors in the range of 30 pW/√Hz but are catching up quickly. Fig. 1 compares the development of Schottky diodes and rectifying field effect transistors over the last decades. The noise equivalent power (NEP) of Schottky diodes is stagnating around 1 pW√Hz in the lower THz range (< 600 GHz) because technological limits are reached. FETs are yet improving very fast.

In this paper, we focus on rectifying FETs tailored to specific applications. The lowest NEP values in Fig. 1 have been achieved with resonant, narrow band antennas or by matching to a waveguide for both Schottky diodes and FETs. For many applications, however, this narrow band operation scheme is disadvantageous. Particularly for spectroscopic applications, a large tuning range is important. We therefore attached FETs to broadband antennas strongly increasing the detection bandwidth.

With a second design, we couple a transistor to two orthogonal dipole antennas in order to achieve mixing and homodyne detection between two orthogonally polarized THz signals.

A third layout works without any antenna. In this case, the THz radiation couples directly to the transistor. This results in an orders of magnitude shorter detector time constant, however, at cost of responsivity. Due to the large size, it is well suited for ultrafast detection of high power THz signals, e.g. generated by a free electron laser, since the THz power can be distributed over the whole area.

2. DETECTION PRINCIPLE

The rectification in FETs originates from simultaneous modulation of the carrier velocity $v(U_{THz})$ by a source-drain THz bias, and the carrier concentration, $n^{(2D)}(U_{THz})$ by the gate-channel bias originating from the same THz signal. The THz bias, $U_{THz}(t) = U_{THz,0}\cos(\omega t)$, results from an incident THz field which is either coupled to a lumped element FET with an antenna or by directly illuminating a large area device (of the order of the THz spot size) with a THz wave. The rectification process remains highly efficient even orders of magnitude above the current and power amplification 3 dB frequencies f_τ and f_{max} [25,26]. In the most general case, a non-linear Euler equation has to be solved to obtain the source-drain bias generated by the device. Since $j(t)=en^{(2D)}(t)v(t)$, the simultaneous modulation of $n^{(2D)}(t)$ and $v(t)$ always produces a term that is proportional to $(U_{THz}(t))^2 = ½\ (U_{THz,0})^2(1+\cos(2\omega t))$, providing a DC component as a detection signal. The exact response of the device, however, depends on the details of the electron transport in the gated region of the transistor. The case of slowly decaying plasmons, where the (momentum) relaxation time, τ, is much longer than the inverse of the THz angular frequency, $\omega\tau >> 1$, is defined as the resonant limit. Plasmons spread far into the gated region and are only weakly damped due to the small relaxation time. They may oscillate under the gate which acts as a plasmonic cavity. Resonant detection requires high THz frequencies at room temperature. For intrinsic GaAs with an electron mobility of μ=8000 cm²/Vs and an effective electron mass of $m^*=0.067m_0$, the criterion $\omega\tau = 2\pi\nu\mu m^*/e > 1$ is fulfilled for ν>0.5 THz. In this paper, however, we will mainly discuss non-resonant detectors, either operated below 0.5 THz or detectors with a long gate where plasma waves are strongly damped within one round trip. The detectors are therefore quasi non-resonant. Detailed theoretical discussion on the detection process can be found elsewhere [25,26].

3. EXPERIMENTAL RESULTS

The samples used in this paper are remotely doped high electron mobility transistors, based on the AlGaAs or InAlGaAs material system. A typical sample structure is illustrated in Fig. 2. The delta doping layer in the barrier (width b~30-65 nm) is fully ionized. The carriers compensate surface charges and accumulate as two dimensional electron gas (2DEG) in the channel that dips under the Fermi energy. Due to the spatial separation of dopants and undoped channel, the carriers show an extremely high mobility. Typical values for the mobility at room temperature are 6000-8000 cm²/(Vs) for (Al)GaAs structures and even up to 10000 cm²/(Vs) for In(Al)GaAs samples. These values are about 25-40 times higher than in silicon-based devices. For most samples studied here, the channel carrier concentration is in the range of 5-7 $x10^{11}$ /cm². The geometrical layout is illustrated in Fig.2 b). Source and drain contacts consist of ohmic Ge/Au/Ni/Au

[2] For Schottky diodes, several values had to be calculated from mixing NEPs since Schottky diodes are mostly implemented as mixers.

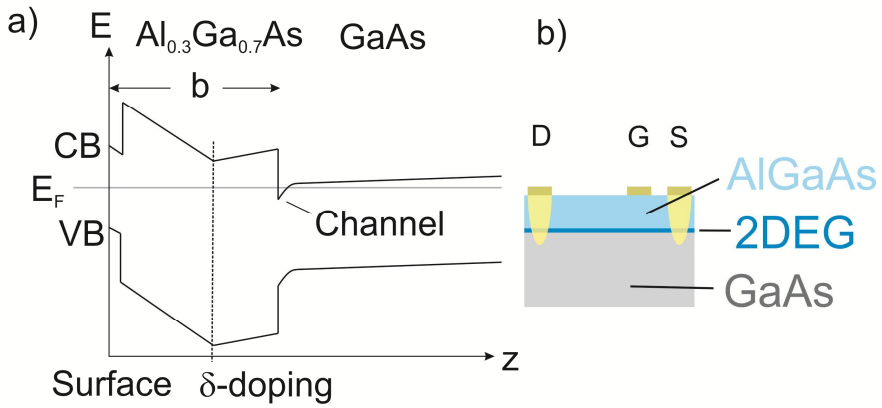

Fig. 2: a) Band diagram of an (Al)GaAs high electron mobility transistor. b) Side view. The antenna is either coupled to source and drain or to source and gate. The gate is positioned closer to source in order to break the symmetry of the device.

contacts and are annealed at 430°C. The Ti/Au Schottky gate contact is deposited closer to one of the ohmic contacts which we define as source contact. This breaks the symmetry of the device. For a symmetrical device with a symmetrical feed of the THz signal (i.e. antenna at source and drain), the rectification at the drain side of the gate cancels the rectified signal at the source side of the gate resulting in no net read out bias [29]. By biasing of the sample with a gate bias, the asymmetry can be altered: Fig. 3 shows THz responsivity measurements around 300 GHz vs. gate bias. The responsivity features a zero crossing at a source-gate bias of -1.4 V. The sign of the read out bias flips at this gate bias, showing that the rectification at the opposite side of the gate dominates at higher biases.

Fig. 3 also shows measurements at 300 GHz where a FET was operated at a finite DC source-drain current. Nadar et al. in ref. [28] demonstrated that the device responsivity can be strongly increased by DC biasing the source-drain port. Here, we operated the SD port in a constant current mode. We find an increase of the responsivity of more than a factor of 100 as compared to zero current operation. The maximum responsivity is 260 V/W with a broadband logarithmic-periodic antenna. For operation with a resonant antenna, we expect a further improvement by a factor of ~4, resulting in a device responsivity of the order of 1 kV/W. The devices were attached to logarithmic-periodic antennas with a design frequency from 60 to 680 GHz, allowing for broadband operation. With an low-frequency optimized device with a gate length of 0.75 µm, we have measured an NEP of 180±30 pW/√Hz at 0.1 THz and zero source-drain bias with a broadband

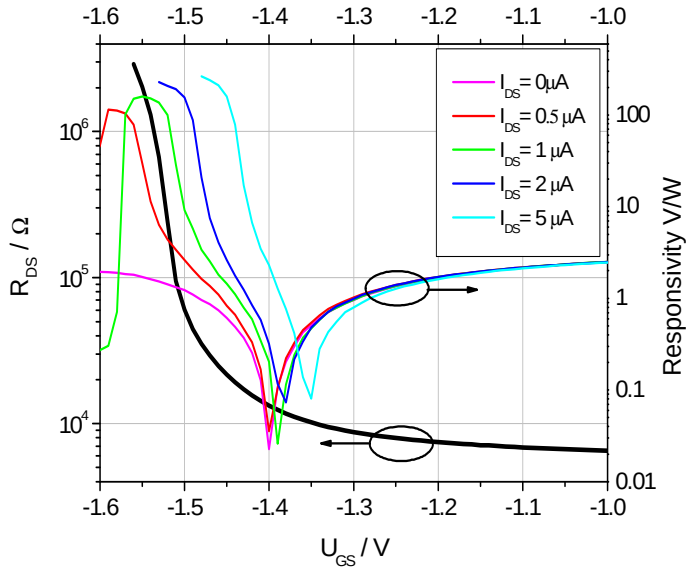

Fig.3: Responsivity and source-drain resistance vs. gate bias. The zero crossing of the responsivity around UGS=-1.4 V is due to symmetrical operation of the FET. At a moderate current of I_{DS}=5 µA, the responsivity was increased by more than a factor of 100 to 260 V/W.

logarithmic-periodic antenna. The responsivity is 80 ±5 V/W. These values are not corrected for any coupling losses, imperfect antennas, and the reflection of the silicon lens. The responsivity of the device decreased strongly with increasing frequency, attributed to a fairly large access resistance of the order of 600 Ω. This results in an RC roll-off of the device. Furthermore, the gate length must be reduced for optimization for higher THz frequencies: At higher frequencies, the rectification happens at shorter length scales [25]. The remaining part of the gated channel contributes to the access resistance. Since the devices have to be operated fairly close to threshold for optimum signal to noise ratio, the contribution of the remaining part of the gated channel to the access resistance is large.

In contrast to silicon-based devices, the carriers do not freeze out at low temperatures since the (Al)GaAs FETs are remotely doped high electron mobility transistors, where ionized dopants and carriers are spatially separated and cannot recombine. In fact, the carrier mobility increases drastically and the gate control of the channel improves since perturbing traps in the barrier cannot be charged any more and gate leakage decreases. This results in an improved responsivity at low temperatures, in addition to reduced thermal noise. Furthermore, ballistic effects and plasmonic resonances increase the responsivity. For an In(Al)GaAs based device, we found an improvement of the responsivity at 5 K of a factor of 8 as compared to operation at room temperature.

We developed a homodyne multiplicative mixer based on a FET rectifier. The mixer consists of a symmetric FET that is coupled to two orthogonal dipole antennas. The first antenna is coupled to the source-drain port, the second antenna is coupled to the source-gate port as illustrated in Fig. 4. The structure is excited with two orthogonally polarized continuous-wave THz signals. The signals are generated by the same THz source, split into two, orthogonally polarized, and subsequently combined by a beam splitter (BS). For lock-in detection, one of the beams is chopped. We define this beam as the signal (S), whereas the unmodulated beam acts as local oscillator (LO). For most measurements, we chopped the signal that is coupled to the source-gate port. However, the detection works also for the alternative excitation where the source-drain signal is modulated and the source-gate signal remains unchopped. The two antennas convert the THz signal to a THz bias. The sample provides a rectified source-drain bias, U_r, according to [29]

$$U_r \sim \left(2U_{GS}^{THz}U_{DS}^{THz}\cos\varphi - \left(U_{DS}^{THz}\right)^2\right), \qquad (1)$$

where φ is the relative phase between DS and GS signals. If only the gate-source signal, U_{GS}, is modulated, only the first part of eq. 1 (i.e. the multiplicative mixing) will be measured by the lock-in amplifier since the second part (direct detection) remains unmodulated. The read out bias is also dependent on the relative phase, φ, between LO and S signals. The responsivity dependence on the relative phase between the two signals shown in

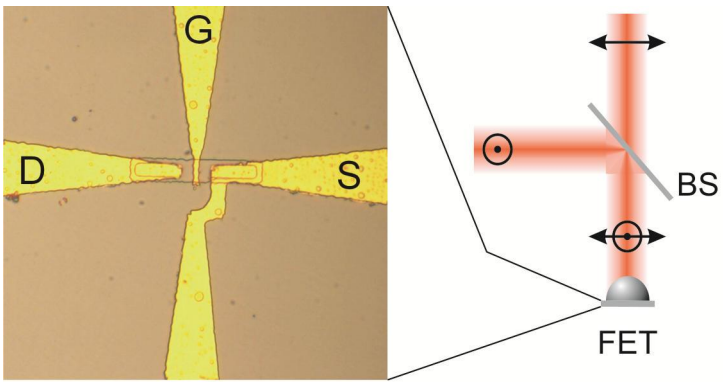

Fig. 4: Setup of the mixing experiment. Two perpendicularly polarized THz signals of same polarization are combined with a beam splitter (BS) and illuminate a FET that is coupled to two sets of orthogonal dipole antennas. One beam excites the source-drain coupled antenna, the other beam the source-gate coupled antenna. A COMSOL multiphysics simulation determined a maximum cross talk of 20 dB between the antennas [29].

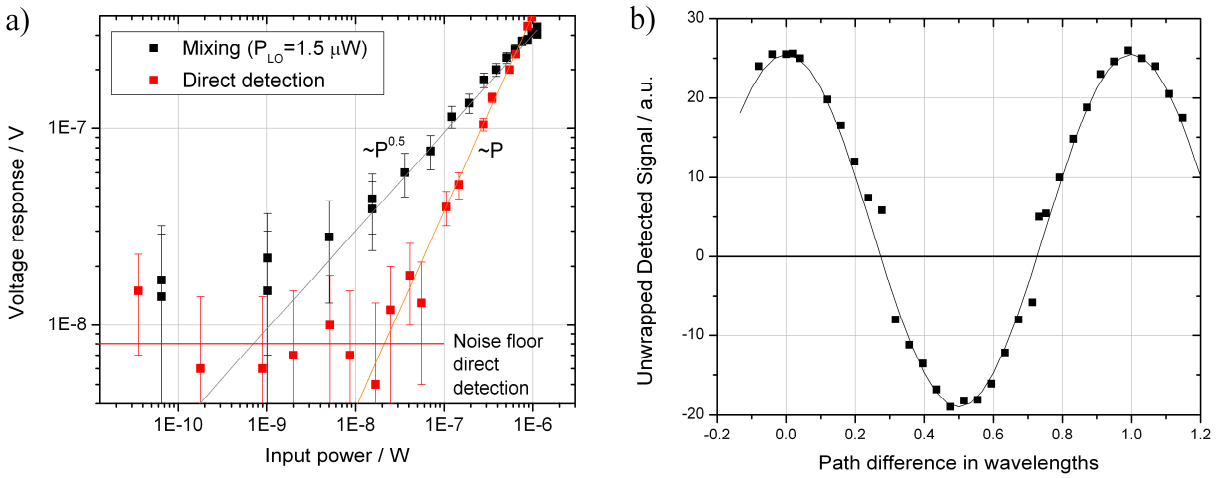

Fig. 5: a) Mixing and direct detection at 570 GHz for sample B. The cross talk is larger for this design, resulting in some direct detection contribution for mixing operation. Since the sample was operated under the condition of equal local oscillator frequency and signal frequency (homodyne operation), mixing and direct detection cannot be distinguished. This leads to the saturation of the lowest detectable power. b) The phase between vertically and horizontally polarized THz beam is altered by a delay stage. As expected for a mixer, the mixing signal is phase sensitive. The solid line represents the theoretical guide for the eye, taking also the static direct detection contribution into account.

Fig. 5 b) proves this mixing operation. The unmodulated (LO) signal was delayed by a mechanical delay line with respect to the signal, S. Two designs were investigated. The first design (sample A) was optimized for operation around 370 GHz, the second design (sample B) for operation around 570 GHz. The FET can also be used as direct detector if only a modulated DS signal is incident on the structure and a small gate bias breaks the device symmetry (see Fig. 5 a). First results and theory are summarized in ref. [29].

For sample B, we determined a lowest detectable power under mixing conditions of 24 nW/Hz at 1.5 µW LO power and a direct detection NEP of 70 nW/√Hz, both at 570 GHz (see Fig. 5 a). The lowest detectable power, however, is not the mixing NEP since cross talk within the structure and reflections within the system lead to a static contribution. Under homodyne conditions ($\nu_{LO}=\nu_S$) a direct detection contribution due to cross talk cannot be distinguished from the mixing signal. Therefore, the detected mixing signal in Fig. 5 a) does not follow the square root dependence at the lowest power levels but rather saturates before it reaches the noise equivalent voltage of ~8 nV. A heterodyne measurement would be required in order to determine the mixing NEP where the mixing contribution appears at another intermediate frequency than the direct detection signal. From the direct detection noise floor, we estimate a mixing NEP of 6 nW/Hz at 1.5 µW LO power.

Results for the low frequency design (sample A, ~370 GHz) are summarized in ref. [29]. We found a mixing NEP of 0.96 nW/Hz at a LO power of 8 µW, a direct detection NEP of 130 nW/√Hz and a responsivity of R=0.41 V/W at 373 GHz. The cross talk was significantly less than for the 570 GHz design. The NEPs at both frequencies are very similar. The fairly high values for the NEPs are due to the large access resistance of the samples. The channel resistance at 0V was already 9.3 kΩ (sample A), attributed to large ungated parts of the device and contact resistance of the ohmic source and drain contacts. From the carrier concentration and mobility obtained by Hall measurements, we estimate that the access resistance is in the range of 8 kΩ. At a gate bias of U_{GS}=-0.65 V(U_G=0.6V), the source-drain resistance increased to 18 kΩ. From ref. [25] eq. 7, we estimate that the RC roll-off results in losses of about $\eta_{RC}=1.2\text{x } 10^{-4}$ at 373 GHz (calculated channel resistance per unit length at U_{GS}=-0.65 V is r_0=170 MΩ/m, channel capacitance per unit length c_0=10.6 nF/m). We note that the RC losses are calculated based on a simplified transistor model. More realistic models such as those in ref. [30] may provide even larger losses. Furthermore, the simulated antenna radiation resistance of 540 Ω is much smaller than the device resistance of 18 kΩ. This results in strong impedance mismatch, further reducing the device efficiency. For a (hypothetic) antenna with a radiation resistance of 18 kΩ, equalling the device resistance, we estimate an improvement of the device efficiency by a factor of 8.9 according to eq. 20 of ref. [25]. The intrinsic responsivity of the FET is therefore R^i=0.41 V/W x 8.9/1.2x 10^{-4} =30 kV/W and the intrinsic direct detection NEP is NEP^i= 130 nW/√Hz /8.9 x 1.2x10^{-4} =1.7 pW/√Hz. This is comparable to state-of-the art Schottky diodes and other results from rectifying field effect transistors.

For most tabletop experiments, low NEP is of crucial importance. However, there are also experiments where ultra-short response time is more important than NEP, particularly, when high speed data acquisition is required. A whole class of such experiments is the study of (ultra-) fast phenomena in matter. Such experiments are often carried out at high power THz facilities such as free electron lasers (FELs). We therefore develop high speed FET-based detectors [31,32] that are able to withstand extraordinarily high THz power levels of FELs (tens of kW peak power at least, average power of several W). A schematic layout of the sample is illustrated in Fig. 6 a) and b). The detector consists of an array of very wide (width=axis perpendicular to the source-drain direction ~100 µm-1 mm) FETs. The array elements are connected in parallel in order to reduce the (parasitic) resistance of the device and, hence, any post-detection RC time originating from the device resistance and the input impedance of the read out electronics such as an oscilloscope. The large area field effect transistor (LA-FET) array may cover an area in the range of 100 x 100 µm up to 1 x 1 mm². Instead of using an antenna, the THz field couples directly to the FET structure: The THz field component that is aligned along the source-drain direction generates a source drain and a source-gate bias, resulting in rectification, similar to the antenna-coupled version. Since no antennas are used and the large area shows a very low radiation resistance (typically < 1 Ω [4]), the responsivity is much smaller than that of antenna-coupled devices. However, the small radiation resistance also ensures a small RC-time constant of the detector, allowing for ultrafast data acquisition. In order to improve the coupling efficiency of the THz power, the array may be mounted on a hyper-hemispherical silicon lens as illustrated in Fig. 6 a).
For read out, the array is coupled to a coaxial cable that feeds a 30 GHz oscilloscope (Tectronix DSA 8200). In order to determine the response time of the LA-FET, it is excited with a few ps (<5 ps) FEL pulse. The response shown in Fig. 6 c) is already limited by the oscilloscope rise time: The half width at half maximum (HWHM) is 20±10 ps, very close to the oscilloscope rise time of 17 ps. The ringing and the reflection at 830 ps is most likely due to imperfect wiring of the device.
Since no antennas are used, there are no resonances, resulting in broadband detection. LA-FETs were successfully characterized from 240 GHz [31] up to 5 THz [32] at two FELs.
Besides high speed, a further advantage of the GaAs-based LA-FET is its sensitivity to 800 nm NIR light. This is particularly important for a whole class of experiments carried out at high THz power facilities such as free electron lasers (FELs): pump and probe experiments. In such experiments, an optical pump beam excites a sample under test. A

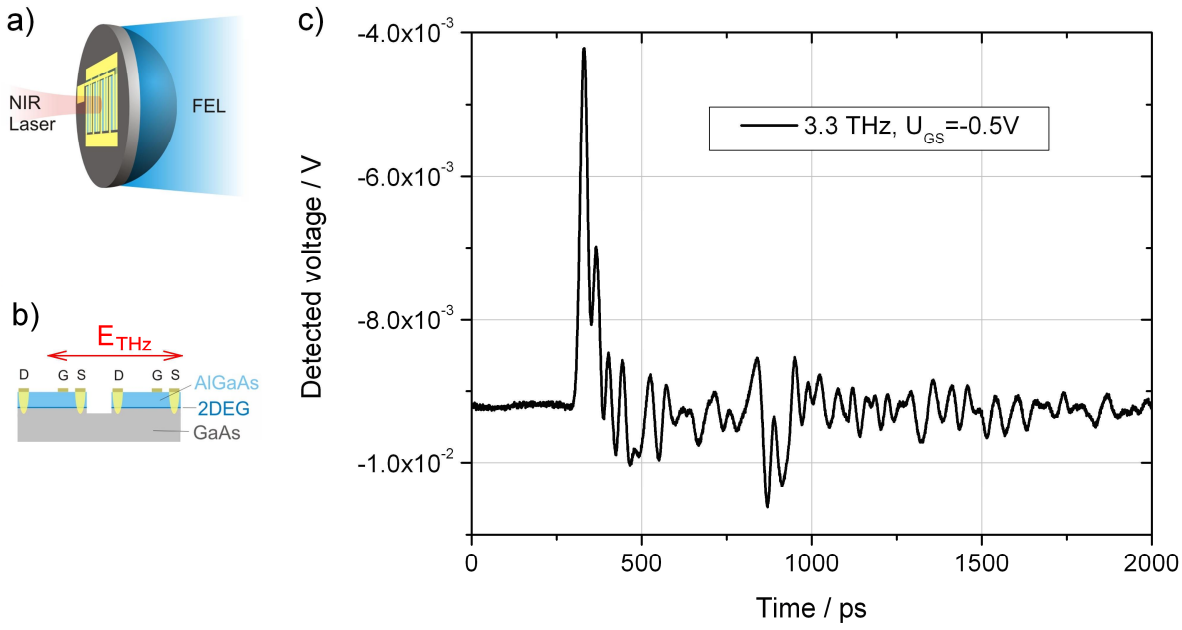

Fig. 6: a) Layout of the large area detector. It is mounted on a silicon lens that collimates the THz power on a 345 x345 µm² device. The device consists of an array of long and narrow asymmetric FETs [31,32]. The device has to be excited with a THz polarization as indicated in b). c) Measurement of a few ps FEL pulse at 3.3 THz with a 30 GHz oscilloscope. The HWHM of 20 ±10 ps of the detected pulse is in the range of the rise time of the oscilloscope.

synchronized THz beam probes the sample with a certain time delay. Recently, also the inverted experiment, i.e. a THz pump and an optical probe became an interesting tool for studying ultrafast dynamics in matter. For tabletop systems such as THz time-domain systems, the synchronization is very simple because the THz beam is generated by the same optical beam that is used for pumping the sample under test. There is no time jitter between the pulses. For FELs, however, there is no natural synchronization. The pump laser and the FEL are independent entities that may also drift and jitter. In order to align pump and probe experiments, a fast detector is required that is able to detect and resolve optical and THz pulses at the same time. The LA-FET is an ideal detector for time-resolved measurements of both THz and NIR pulses. We achieved a resolution of the NIR pulse of ~100 ps. Further details synchronous NIR and THz detection with LA-FETs can be found in ref. [32].

4. SUMMARY

We have summarized several broadband detector layouts using GaAs-based field effect transistor rectifiers. We have shown that broadband detection (~60 GHz -680 GHz) can be achieved by coupling a FET to a broadband logarithmic-periodic antenna. The FET was optimized for low frequencies, resulting in a measured NEP of 180 pW/√Hz at 100 GHz. The NEP increased with increasing frequency since shorter gates and reduced access resistance is required for optimized performance at higher frequencies. We introduced another broadband concept that does not use antennas: The large area field effect transistor (LA-FET). It consists of an array of very wide FETs. We have shown that LA-FETs can be extremely fast, reaching detection time constants in the range of 20 ps. This value is already limited by the post detection electronics. We further have shown results on a narrow band THz mixer that mixes two orthogonally polarized THz signals that are coupled to the source-drain port and to the source-gate port respectively. Multiplicative mixing under homodyne detection conditions has been demonstrated at 370 GHz and 570 GHz.

ACKOWLEDGEMENTS

H. Lu, P. G. Burke and A. C. Gossard acknowledge funding from the U.S. Intelligence Advanced Research Projects Activity (IARPA), through the U.S. Army Research Office. S. Kim and S. Preu acknowledge funding from the Air Force Office of Scientific Research via STTR Contract FA9550-10-C-0177. S. Preu acknowledges funding from the Humboldt foundation.

REFERENCES

[1] H. H. Mantsch and D. Naumann, "Terahertz spectroscopy: The renaissance of far infrared spectroscopy," Journal of Molecular Structure **964**, 1–4, (2010)

[2] F. Matsushima, H. Nagase, T. Nakauchi, H. Odashima, and K. Takagi, "Frequency measurement of pure rotational transitions of $H_2{}^{17}O$ and $H_2{}^{18}O$ from 0.5 to 5 THz," J. of Mol. Spectroscopy **193**, 217–223 (1999)

[3] L. Ho, M. Pepper, and P. Taday, "Terahertz spectroscopy: Signatures and fingerprints," Nature Photon. **2**, 541–543 (2008)

[4] S. Preu, G. H. Döhler, S. Malzer, L.J. Wang, and A. C. Gossard, "Tunable, continuous-wave Terahertz photomixer sources and applications," J. Appl. Phys. **109**, 061301 (2011).

[5] C. Sydlo, O. Cojocari, D. Schönherr, T. Goebel, S. Jatta, H. L. Hartnagel, and P. Meissner, "Ultrawideband THz detection based on a zero-bias Schottky diode," 19th Int. Symp. On Space THz Technol., 520 (2008)

[6] J. L. Hesler, and T. W. Crowe, "Responsivity and noise measurements of zero-bias Schottky diode detectors, " Proc. of 18th Int. Symp. on Space THz Technol. **89,** (2007)

[7] D. T. Hodges and M. McColl, "Extension of the Schottky barrier detector to 70 μm (4.3 THz) using submicron-dimensional contacts," Appl. Phys. Lett. **30**, 5-7 (1977)

[8] H. P. Röser, E. J. Durwen, R. Wattenbach, and G. V. Schultz, "Investigation of a heterodyne receiver with open structure mixer at 324 GHz and 693 GHz," Int. J. of Infrared and MM waves, **5**, 301-314 (1984)

[9] V. V. Kubarev, G. M. Kazakevitch, Y. U. Yeong, and B. C. Lee, "Quasi-optical highly sensitive Schottky-barrier detector for a wide-band FIR FEL," Nuc. Instr. & Methods Phys. Res. A **507**, 523-526, (2003)

[10] E.R. Brown, A. C. Young, J. E. Bjarnason, J. D. Zimmerman, and A. C. Gossard, "Millimeter and sub-millimeter wave performance of an ErAs:InGaAs Schottky diode coupled to a single turn square spiral," Int. J. High Speed Electron. **17**, 383-394 (2007)
[11] R. Han, Y. Zhang, D. Coquillat, H. Videlier, W. Knap, E. Brown, and O K. K. "A 280-GHz Schottky diode detector in 130-nm digital CMOS," IEEE Solid-State Circ. **46**, 2602-2612 (2011)
[12] L. Liu, J. L. Hesler, H. Xu, A. W. Lichtenberger, and R. M. Weikle,. "A broadband quasi-optical terahertz detector utilizing zero bias Schottky diode," IEEE Microw. Wirel. Compon. Lett. **20**, 504-506 (2010)
[13] K. Mizuno, R. Kuwahara, and S. Ono, "Submillimeter detection using a Schottky diode with a long wire antenna," Appl. Phys. Lett. **26**, 605-607 (1975)
[14] N. C. Luhmann and W. A. Peebles, "Instrumentation for magnetically confined fusion plasma diagnostics," Rev. Sci. Instrum. **55**, 279-33 (1984)
[15] A. El Fatimy, J. C. Delagnes, A. Younus, E. Nguema, F. Teppe, W. Knap, E. Abraham, and P. Mounaix, "Plasma wave field effect transistor as a resonant detector for 1 Terahertz imaging applications," Optics Commun. **282**, 3055-3058 (2009)
[16] A. El Fatimy, S. Boubanga Tombet, F. Teppe, W. Knap, D. B. Veksler, S. Rumyantsev, M. S. Shur, N. Pala, R. Gaska, Q. Fareed, X. Hu, D. Seliuta, G. Valusis, C. Gaquiere, D. Theron, and A. Cappy, "Terahertz detection by GaN/AlGaN transistors," Electron. Lett. **23,** 1342-1343 (2006)
[17] E. Öjefors, U.R. Pfeiffer, A. Lisauskas, and H. G. Roskos, "A 0.65 THz focal-plane array in a quarter-micron CMOS process technology," IEEE J. Solid-State Circuits, **44**, 1968-1976 (2009)
[18] Erik Öjefors, Neda Baktash, Yan Zhao, Richard Al Hadi, Hani Sherry, and Ullrich R. Pfeiffer, "Terahertz imaging detectors in a 65-nm CMOS SOI technology," Proc. ESSCIRC, 486-489 (2010)
[19] X. G. Peralta, S. J. Allen, M. C. Wanke, N. E. Har_, M. P. Lilly, J. A. Simmons, J. L. Reno, P. J. Burke, J. P. Eisenstein, W. Knap, Y. Deng, S. Rumyantsev, J.-Q.Lü, and M. S. Shur, "THz detection by resonant 2-D plasmons in field effect devices," Int. J. High Speed Electron. Syst. 1**2**, 925_937 (2002)
[20] E. A. Shaner, M. Lee, M. C. Wanke, A. D. Grine, J. L. Reno, and S. J. Allen, "Tunable THz detector based on a grating gated field-effect transistor," Proc. SPIE **6120**, 612006 (2005)
[21] H. Sherry, R. Al Hadi, J. Grzyb, E. Ojefors, A. Cathelin, A. Kaiser, and U. R. Pfeiffer, "Lens integrated THz imaging arrays in 65nm cmos technologies" IEEE RFIC, 1-4 (2011)
[22] W. Stillman, F. Guarin, V.Yu. Kachorovskii, N. Pala, S. Ryumantsev, M. S. Shur, and D. Veksler, "Nanometer scale complementary silicon MOSFET as detector of terahertz and sub-terahertz radiation," IEEE Sensors 2007, 934_937 (2007)
[23] J. D. Sun, F. Y. Sun, D. M. Wu, Y. Cai, H. Qin, and B. S. Zhang, "High-responsivity, low noise, room-temperature, self-mixing terahertz detector realized using floating antennas on a GaN-based field-effect transistor," Appl. Phys. Lett. **100**, 013506 (2012)
[24] W. Knap, F. Teppe. N. Dyakonova, D. Coquillat, and J. Lusakowski, "Plasma-wave oscillations in nanometer field effect transistors for terahertz detection and emission," J. of Physics **20**, 384205 (2008)
[25] S. Preu, S. Kim, R. Verma, P. G. Burke, M. S. Sherwin, and A. C. Gossard, "An improved model for nonresonant terahertz detection in field-effect transistors," J. Appl. Phys. **111**, 024502 (2012)
[26] D. Veksler, F. Teppe, A. P. Dmitriev, V. Y. Kachorovskii, W. Knap and M. S. Shur, "Detection of terahertz radiation in gate two-dimensional structures goverend by dc current," Phys. Rev. B **73**, 125328 (2006)
[27] V. V. Popov, D. V. Fateev, T. Otsuji, Y.M. Meziani, D. Coquillat, and W. Knap, "Plasmonic Terahertz detection by a double-grating-gate field effect transistor structure with an asymmetric unit cell," Appl. Phys. Lett. **99**, 243504 (2011)
[28] S. Nadar, H. Videlier, D. Coquillat, F. Teppe, M. Sakowicz, N. Dyakonova, W. Knap, D. Seliuta, I. Kašalynas, and G. Valušis, "Room temperature imaging at 1.63 and 2.54 THz with field effect transistor detectors," J. Appl. Phys. **108**, 054508 (2010)
[29] S. Preu, S. Kim, R. Verma, P.G. Burke, N. Q. Vinh, M. S. Sherwin, und A. C. Gossard, "Terahertz detection by a homodyne field effect transistor multiplicative mixer," IEEE Trans. THz Sci. Technol. **2**, 278-283 (2012)
[30] Y. Tsividis and C. McAndrew, *Operation and Modeling of the MOS Transistor*, Oxford University Press (2011)
[31] S. Preu, H. Lu, M. S. Sherwin, und A. C. Gossard, "Detection of nanosecond-scale, high power THz pulses with a field effect transistor, " Rev. Sci. Instrum. **83**, 053101 (2012)
[32] S. Preu, M. Mittendorff, S. Winnerl, H. Lu, A. C. Gossard, H. B. Weber, "Ultra-fast transistor-based detectors for precise timing of near infrared and THz signals,**"** Opt. Express **21**, 17941-17950 (2013)

[33] P. Földesy, “Current steering detection scheme of three terminal antenna-coupled field effect transistor detectors,” Opt. Lett. 38, 2804-2806 (2013)
[34] G.C. Dyer, G. R. Aizin, S. Preu, N. Q. Vinh, S. J. Allen, J. L. Reno, and E. A Shaner, “Inducing an Incipient Terahertz Finite Plasmonic Crystal in Coupled Two Dimensional Plasmonic Cavities,” Phys. Rev. Lett. **109**, 126803 (2012)